

# The Hubble Constant from Type Ia Supernovae in Early-Type Galaxies <sup>\*</sup>

Tom Richtler<sup>1</sup> and Georg Drenkhahn<sup>2,1</sup>

<sup>1</sup> Sternwarte der Universität Bonn, Auf dem Hügel 71, 53121 Bonn, Germany

<sup>2</sup> Max-Planck-Institut für Astrophysik, Karl-Schwarzschild-Str. 1, 85740 Garching, Germany

**Abstract.** Type Ia supernovae (SNe) are the best standard candles available today in spite of an appreciable intrinsic variation of their luminosities at maximum phase, and of probably non-uniform progenitors. For an unbiased use of type Ia SNe as distance indicators it is important to know accurately how the decline rate and colour at maximum phase correlate with the peak brightness. In order to calibrate the Hubble diagram of type Ia SNe, i.e. to derive the Hubble constant, one needs to determine the absolute brightness of nearby type Ia SNe. Globular cluster systems of early type Ia host galaxies provide suitable distance indicators. We discuss how Ia SNe can be calibrated and explain the method of Globular Cluster Luminosity Functions (GCLFs). At present, the distance to the Fornax galaxy cluster is most important for deriving the Hubble constant. Our present data indicate a Hubble constant of  $H_0 = 72 \pm 4 \text{ km s}^{-1} \text{ Mpc}^{-1}$ .

As an appendix, we summarise what is known about absolute magnitudes of Ia's in late-type galaxies.

## 1 Introduction

### 1.1 Supernova Classification

When the “new” star in Andromeda appeared in 1885 with its striking association with the Great Andromeda Nebula, it was still a long way to go until the recognition that these phenomena represent, like nothing else, our deep relation with the Universe. Shortly after 1920, astronomers learned that the Andromeda nebula was located far outside our Milky Way and that the “Nova” S Andromedae must have been much more luminous than any other nova. Thus Fritz Zwicky created the term *supernova* (SN) for these events, of which by 1930 only a handful had been detected in external galaxies.

Today it is common wisdom that supernovae are largely responsible for the enrichment of the universe with heavy elements and thus also enable the existence of life. Supernova detections are no longer a matter of incident alone: Sophisticated supernova searches with automatic telescopes are now routinely conducted and, thanks to these efforts, we have detected 1387 SN events until February 1999.

<sup>\*</sup> To be published in: Kundt W., van de Bruck C. (Eds.) *Cosmology and Astrophysics: A collection of critical thoughts. Lecture Notes in Physics*, Springer

Morphological classification is one of the first scientific steps on the way to the understanding of a new phenomenon. It is amazing that the first attempts to classify SNe still provide the basis, although our classification scheme has become more subtle and we now know that the morphological phenomenon “Supernova” embraces physically distinct processes (for the early years see the excellent review of Trimble [56], a recent review on SNe Ia as distance indicators is from Branch [7]).

As did Minkowski in 1936, we still basically distinguish two types of SNe, types I and II. This classification is purely spectroscopic: type I events do not show hydrogen lines in their spectra, while type II events do so. An important observation can be made with respect to the parent population of SNe: type I appears in all sorts of galaxies, while type II seems to be restricted to galaxies with a young stellar population, i.e. spiral galaxies and irregulars. For many years, the canonical interpretation was that the progenitors of type I stem from an old stellar population. A popular model is a matter-accreting white dwarf in a binary system which becomes unstable when the Chandrasekhar mass limit is reached. Then the star explodes by thermonuclear detonation or deflagration [64] (which is just another expression for super- or subsonic movement of the burning front but is nevertheless very important in modelling the event), but see Kundt [29] for difficulties of this model. On the other hand, type II was thought to be the explosion of a massive star, whose core collapses at the end of its evolution, forms a neutron star (already Zwicky had this vision), and the released gravitational energy (about  $10^{53}$  erg) drives the expansion of the outer shells (in a complicated and not yet fully understood manner). Regarding the energetics of type II events, it soon became clear that radiation and the kinetic energy of the shell must be only a tiny fraction of the total energy ( $10^{51}$  erg), the rest being emitted as neutrinos. The detection of neutrinos from SN 1987A was a triumph to this theory (e.g. [31]).

The coarse classification depending on the spectral hydrogen features is further refined. The subclassification of type II by the shape of the light curve appears useful, distinguishing SNe II with (II $p$  for  $p$ lateau) or without plateaus (II $l$  for  $l$ inear), which basically depends on the thickness of the hydrogen shell and the speed at which the H-ionisation front moves inward during expansion. But type I SNe are also subclassified into Ia, Ib and Ic. By 1983, a few type I SNe had been observed which developed strong radio emission a few weeks after maximum light. This is now commonly interpreted as the core collapse and subsequent explosion of the outer layers of a massive evolved star (for instance a Wolf-Rayet star) which lost its hydrogen shell prior to the explosion. This new type of SN without hydrogen lines and massive progenitor was named Ib or Ic, depending on whether helium lines were strong or not. The remaining type Ia is spectroscopically distinct from Ib by the occurrence of Si lines in an otherwise very similar spectrum.

For more information on SN classification refer to Wheeler & Harkness [62] and Filippenko [12].

## 1.2 The parent population of type Ia SNe

In a modern compilation (Asiago catalogue [4]), we now have 403 classified Ia events at the time of writing (May 1999). Their distribution among the host galaxies is shown in Fig. 1. The abscissa is de Vaucouleurs' classification, where the extreme numbers are  $-5$  (elliptical galaxies) and  $10$  (late-type irregulars). It is apparent that Ia in elliptical galaxies are rarer than in spiral galaxies. If we normalise to luminosity, then the difference becomes even more obvious.

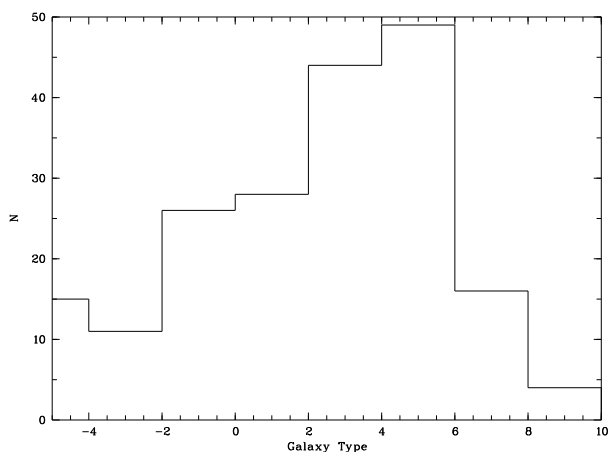


**Fig. 1.** Distribution of type Ia SNe depending on the host galaxy type (de Vaucouleurs' classification). It is apparent that Ia events in early-type galaxies are rarer than in late-type galaxies.

Table 1 shows the SN Ia rate in different galaxy types according to Cappellaro et al. [8]. If we recall that a typical  $(M/L)_V$ -ratio in elliptical galaxies is about 8 and in spiral galaxies about 0.05, then it becomes clear that a unit mass in spiral galaxies produces many more SNe than in elliptical galaxies. This would be understandable if spiral galaxies had more opportunities to let Ia's explode than elliptical galaxies have. Indeed, the former hypothesis, that all Ia's are explosions of Chandrasekhar mass white dwarfs in old population environments, now stands on very weak grounds. Recent investigations have revealed that there exists a weak statistical correlation with spiral arms in spiral galaxies [5], which speaks in favour of the contribution of a parent population of massive stars for at least some Ia's. On

the other hand, in elliptical galaxies, at best very few massive stars exist, so one is driven towards the conclusion that Ia's originate in young *and* old populations. A further, quite irritating observation is that Ia's seem to avoid the central regions of ellipticals and spirals [61], so that the old bulge populations apparently are not effective producers of Ia events. Some researchers even propose that every supernovae has a massive progenitor, e.g. Kundt [28].

However, our theme is not the physics of Ia's but how they can be exploited to obtain the Hubble constant. In the next section, we shall see that in spite of a probably non-uniform origin, Ia's exhibit stunningly homogeneous properties which make them excellent standard candles.

**Table 1.** SN rates for various galaxy types in  $\text{SNu} = \# \text{ of SNe} \times [L_{\text{host gal.}} / (10^{10} L_{\odot}) \cdot t / (100 \text{ yr})]^{-1}$ , according to Cappellaro et al. [8]. Rates in SNu scale as  $(H_0 / (75 \text{ km s}^{-1} \text{ Mpc}^{-1}))^2$

Galaxy Type	Ia rate [SNu]
E-S0	$0.13 \pm 0.06$
S0a-Sb	$0.17 \pm 0.07$
Sbc-Sd	$0.39 \pm 0.19$

## 2 SNe Ia as distance indicators

### 2.1 The light curve

It has long been noted that the overall shapes of SN Ia light curves are surprisingly similar. Figure 2 shows a “typical” light curve. After the maximum, a slow decline follows which has a smooth transition to a linear part. A linear relation between time, which enters linearly, and a logarithmic parameter, magnitude, reflects an exponential law. The suspicion that the light curve is triggered by the decay  $^{56}\text{Ni} \rightarrow ^{56}\text{Co} \rightarrow ^{56}\text{Fe}$  was therefore expressed quite early [9]. Meanwhile, beside the case of SN 1987A [2], there is evidence from the observation of the  $^{56}\text{Co}$  line in several supernovae [27].

### 2.2 The Hubble diagram

If one tried to compare the maximum luminosities of SNe by distance determinations of the respective, necessarily nearby, host galaxies, the error in the distance would probably dominate the scatter in the maximum brightness, unless the accuracy of the distance determination is very high. A better way of assessing the quality of SNe Ia as distance indicators is therefore to plot them in a so-called “Hubble - diagram”, which uses the apparent peak magnitude as ordinate and  $\log cz$  as abscissa, where  $c$  is the speed of light and  $z$

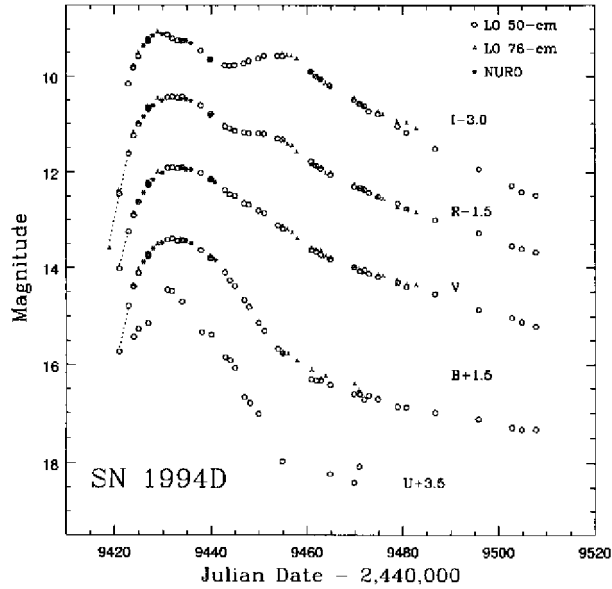


**Fig. 2.** Light curves of SN 1994D [36] in NGC 4526 as an example of typical light-curve shapes of type Ia SNe in the optical passbands.

the redshift of the host galaxy.  $cz$  is sometimes called the ‘recession velocity’ because for small  $z$ , the cosmological expansion is not distinguishable from a Doppler effect.

Figure 3 shows the Hubble diagram for 197 classified Ia SNe, with the heliocentric  $cz$  and the visual apparent maximum magnitude plotted. From  $m - M = 5 \log r - 5$  and the linear approximation of the redshift-distance relation  $cz = H_0 \cdot r$  for small  $z$ , one obtains

$$m = 5 \log cz \underbrace{- 5 \log H_0 + M + 25}_Z. \quad (1)$$

Thus the slope in such a diagram is always 5 while the zero-point  $Z$  is the only free parameter, which has to be fixed by observations like in Fig. 3. Throughout this text, we regard  $cz$ ,  $H_0$  and  $r$  as given in their canonical units, viz.  $\text{kms}^{-1}$ ,  $\text{kms}^{-1} \text{Mpc}^{-1}$  and  $\text{Mpc}$ , respectively. If all Ia’s had the same absolute maximum magnitude  $M$ , the distance and thus the brightness of one SN would principally suffice to determine the Hubble constant:

$$\log H_0 = 0.2 \cdot (M - Z) + 5. \quad (2)$$

In reality, one would of course aim at determining the distance to as many SNe as possible.

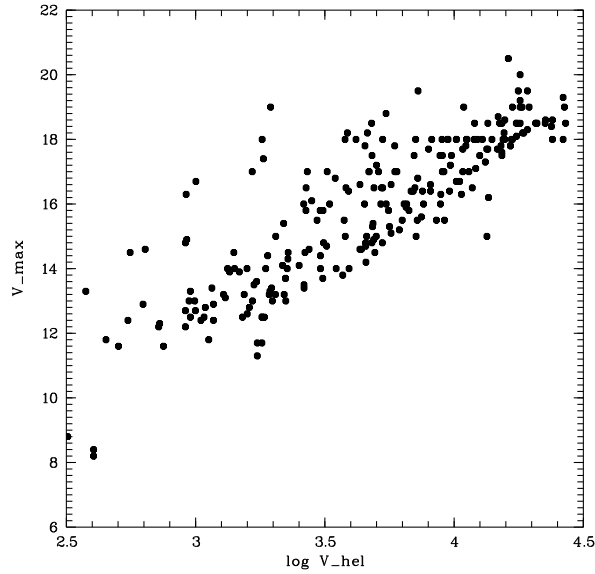


**Fig. 3.** The Hubble diagram from 197 type Ia SNe taken from the Asiago SN catalogue [4]. Plotted is the apparent maximal V-brightness versus the logarithm of the heliocentric recession velocity of the host galaxy.

However, the assumption that all Ia's have the same peak brightness is at first glance not supported by Fig. 3. The dispersion around the mean relation is more than 1 mag and there would be no hope that SNe Ia could be reliable distance indicators (however, note the sharp borderline of the bright side of the distribution). But we must be aware that the sample shown in Fig. 3 is not a careful selection of good, or even excellent, observations. Many SNe have badly determined maxima, we did not correct for extinction, and most of the SNe have been measured in the pre-CCD era, while it may be important to take account of the fact that many SNe are embedded in the irregular structure of their host galaxies. This is only possible with CCD observations. During the 80s and early 90s, the dispersion in the Hubble diagram of SNe could be reduced to typically 0.4 mag, which gave some hope that SNe Ia are indeed good standard candles.

A new level of accuracy was achieved with the publication of the Calán/Tololo sample by Hamuy et al. [18], which contained 29 Ia SNe. These authors performed a coordinated search programme for Ia SNe between 1992 and 1994, with the aim to detect SNe as early as possible, observe good or even excellent light curves in  $B$ ,  $V$  and  $I$  and treat the data in a homogeneous manner. Moreover, they corrected for foreground extinction, applied the  $K$ -correction and referred all redshifts to the rest frame as defined by

the microwave background. Figure 4 shows as an example their Hubble diagram in  $V$ . The scatter is now only 0.26 mag, showing the importance of high-quality CCD observations.

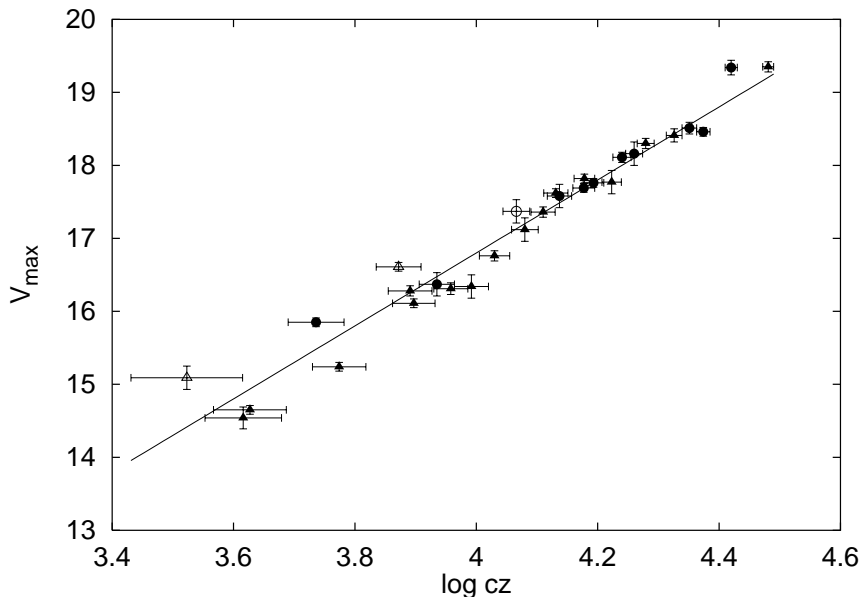


**Fig. 4.** The Hubble diagram from the high quality data of the Calán/Tololo sample in the  $V$  band. Open symbols: red SNe, Triangles: late-type host galaxies, Squares: early-type host galaxies.

But, equally important, it turns out that the scatter around the mean line is *not erratic* but shows a *systematic* behaviour. This sounds strange, but, in fact, was already suspected in the late 70s. The two important parameters are the *decline rate* of a given SN and its *colour* at maximum light. Reviving earlier work, Phillips [34] again collected evidence for the fact that Ia SNe with a slow decline after maximum light are intrinsically brighter than SNe with a fast decline. To put this in quantitative terms, the decline rate  $\Delta m_{15}$  has been defined as the decline in magnitudes of the  $B$  light curve 15 days after maximum light.

Regarding the colour, three intrinsically red SNe are marked by open symbols in Fig. 4. It can be seen that they are atypical. They seem to be too faint in comparison with the ‘normal’ SNe with colours  $B_{\max} - V_{\max} < 0.2$  mag. Note that this red colour and low brightness is not an extinction effect but is rather an intrinsic feature of these three SNe, as will be made plausible later on. The high internal precision of the Calán/Tololo sample of

SNe is a good precondition to investigate further the role of decline rate and colour.

To model the relation between brightness, decline rate and colour, a linear approach like

$$m_{\text{cor}} = m + b \cdot (\Delta m_{15} - 1.1) + R \cdot (B_{\text{max}} - V_{\text{max}}) = 5 \log cz + Z \quad (3)$$

is appropriate. The fit parameters  $b$ ,  $R$  and  $Z$  must then be chosen so that the scatter of the corrected magnitudes  $m_{\text{cor}}$  around a straight line is minimal. Table 2 shows the results of our maximum-likelihood fit for the Calán/Tololo data in  $B$ ,  $V$  and  $I$ .

**Table 2.** The fitted decline rate and colour correction coefficients and zero points for the Hubble diagram of type Ia SNe based on the Calán/Tololo SN sample. The three red SNe from this sample were excluded from the fit to eliminate the influence of any peculiar SN events.

	$B$	$V$	$I$
$b$	$-0.48 \pm 0.23$	$-0.52 \pm 0.19$	$-0.40 \pm 0.22$
$R$	$-1.51 \pm 0.62$	$-0.83 \pm 0.57$	$-0.81 \pm 0.59$
$Z$	$-3.306 \pm 0.063$	$-3.320 \pm 0.058$	$-3.041 \pm 0.060$

To uncover the effects of decline rate and colour, we plot the corresponding magnitude corrections versus decline rate and versus colour. Figure 5 shows the relation between decline rate  $\Delta m_{15}$  and the colour and redshift-corrected  $V$ -magnitude  $V_{\text{max}} - 5 \log cz + R \cdot (B_{\text{max}} - V_{\text{max}})$ . A correlation, in the sense that fast decliners are intrinsically fainter, is clearly visible. Such a behaviour is also theoretically understandable. If the light curve is triggered by the decay of  $^{56}\text{Ni}$ , the available amount of Ni should have a considerable effect. The higher the Ni mass, the brighter the SN, and the longer the time needed for the deposited energy to be radiated away [22]. Figure 6 shows the relation between the colour  $B_{\text{max}} - V_{\text{max}}$ , the decline rate, and the redshift-corrected  $V$ -magnitude  $V_{\text{max}} - 5 \log cz + b \cdot (\Delta m_{15} - 1.1)$ . Because most of the SN colours lie in a small range, the colour correction is smaller than the decline-rate correction. As mentioned earlier, the colour correction accounts for the intrinsic differences of type Ia SNe and not for extinction. Otherwise the correction coefficient  $R = 0.83$  for the  $V$  band would have a value similar to  $A_V/E(B - V) = 3.1$ . But even if the extinction for a given SN is under- or overestimated, the colour correction points in the right direction and weakens any extinction error.

The corrected magnitudes scatter around a straight line only within the measurement uncertainties. Type Ia SNe are therefore not perfect standard candles but almost perfectly *standardisable* candles. Figure 7 shows the amazing reduction of the scatter in the corrected SN magnitudes in comparison with the diagram of uncorrected SN magnitudes in Fig. 4.



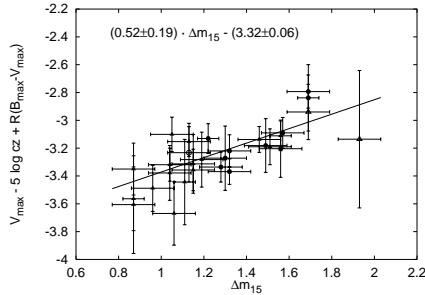


**Fig. 5.** The relation between decline rate and colour-corrected maximum  $V$ -magnitude. The triangles mean SNe in spiral galaxies, the circles mean SNe in early-type galaxies. It is interesting that in spiral galaxies, all kinds of decline rates occur while only fast decliners exist in ellipticals and S0's. This could be indicative of the fact that SNe Ia occur in more than one population.

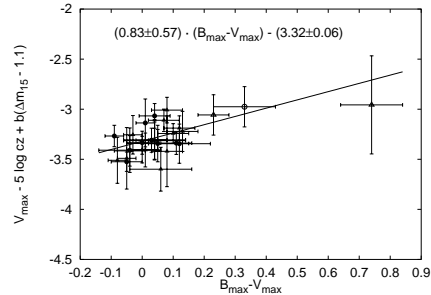


**Fig. 6.** The analogous relation between colour and decline rate-corrected maximum  $V$ -magnitude. The fit is done *without* the three very red SNe. One sees that the relation for normally coloured SNe also applies to the red ones.

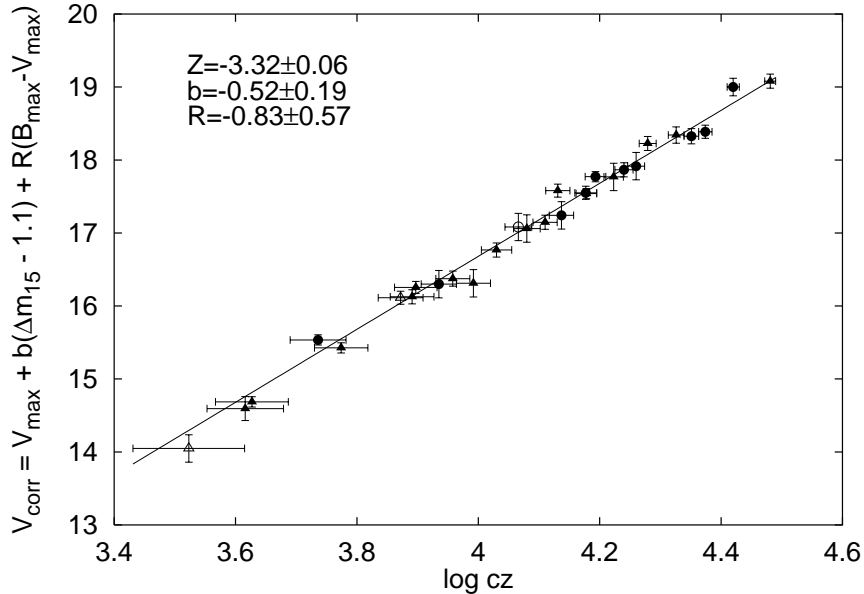


**Fig. 7.** The Hubble diagram of corrected SN magnitudes. The scatter of  $\sigma = 0.15$  mag is fully consistent with the photometric errors and redshift uncertainties as indicated by the error bars, indicating that the *intrinsic* scatter is below the measurement accuracy.

### 3 Globular Cluster Luminosity Functions

The method of distance determination through Globular Cluster Luminosity Functions has revealed itself as a powerful and accurate method to derive distances to elliptical and S0 galaxies. Spiral galaxies are not suitable, because we need *old* globular clusters (GCs), which are fewer in number in spirals than in elliptical galaxies and difficult to detect.

#### 3.1 The principle

The principle is easily explained: the “Globular Cluster Luminosity Function” (GCLF) is simply the distribution function of the apparent or absolute magnitudes of globular clusters. In the literature the term GCLF is often used also for the histogram of the observed GC magnitudes related to a given host galaxy. For example, Fig. 8 shows the GCLF of the Galactic system. We omitted a few clusters due to uncertain extinction corrections. The peak magnitude in the histogram is called the “Turn-Over Magnitude” (TOM). The claim now is that this TOM has a *universal brightness*, which can be calibrated with the Galactic system and which accordingly can serve as a distance indicator. It is important to realise that this TOM does not correspond to any characteristic mass. It is rather a consequence of the fact that the mass function of GCs can be described as  $dN/dm \sim m^{-\eta}$ ,  $dN$  being the number of clusters in the mass interval  $[m, m + dm]$ , with varying exponent  $\eta = \eta(m)$ . The logarithmic binning of magnitude then creates a maximum when the exponent takes the value  $\eta = 1$ , assuming a constant  $M/L$  ratio [32]. It is clear that a universal TOM can exist only among *old* globular cluster systems because the luminosity of young GCs depends strongly on the exact age.

While theoretically not well understood in detail, the empirical evidence for a universal TOM is quite strong. Not only the system of M31, also elliptical galaxies in the Virgo and Fornax galaxy clusters have globular cluster systems (GCSs) whose TOMs, within the observational errors, agree with that of the Milky Way system. Although not completely clear, the physical cause for the existence of a universal TOM is probably the combined effect of a universal mass spectrum of newly formed clusters together with a dynamical erosion of clusters (e.g. [63]). In this context, it is striking that the mass spectrum of molecular clouds in the Milky Way has the same mass spectrum as for instance the mass-rich end of the mass spectra of several elliptical galaxies. If, for any reason, the mass spectrum of molecular clouds is universal and cluster formation inside molecular clouds occurs in a stochastic way (regarding masses) then it is plausible for statistical reasons that the mass spectrum of star clusters reflects the mass spectrum of the parent molecular clouds, if the probability for a certain cluster mass is approximately proportional to the parent cloud’s mass. In this context, it is at least interesting that the mass spectrum of Galactic molecular clouds is well represented by a power

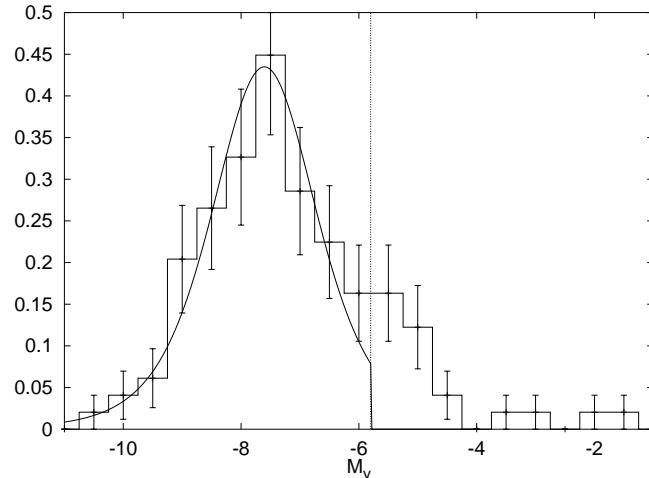


**Fig. 8.** The GCLF of the galactic GCS in the  $V$  band. The vertical line indicates the magnitude where the distribution becomes asymmetric.

law with  $\eta \approx -1.7$  [20,21]. This exponent has also been found for the mass spectrum of globular clusters at high masses (e.g. [63]).

### 3.2 The calibration of the TOM

If we want to measure the absolute brightness of the TOM, we have to know the distances to the Galactic globular clusters. This field has expanded dramatically during the last years and even for specialists it has become increasingly difficult to follow the literature in detail. Of course, distances to globular clusters are not mysterious; what makes it complicated is the demand for *accuracy*.

Distances to globular clusters are normally measured by the brightness of their horizontal branches. This brightness (we take the mean brightness of all HB stars in the  $V$ -band)  $M_V$  depends on metallicity. We write

$$M_V = \alpha \cdot ([\text{Fe}/\text{H}] + 1.6) + \beta. \quad (4)$$

Without exaggerating too much, one can say that the determination of the coefficients  $\alpha$  and especially  $\beta$  is a key to the distance scale, to globular cluster ages, and consequently also to the age of the universe (e.g. [58]). Because we regard the entire globular cluster system, an error in  $\alpha$  does not matter much. If  $\alpha$  is overestimated, clusters of high metallicities will be underestimated in brightness but this will largely be compensated by low-metallicity clusters. That means the error in  $M_V$  and thus in the distance is dominated by the zero-point error in  $\beta$ . Therefore, we adopt the most

recent value for  $\alpha$  from the literature and calibrate the zero-point  $\beta$  with the aid of RR Lyrae stars and horizontal branches of globular clusters in the Large Magellanic Cloud (LMC), which correspondingly becomes our *most important distance standard*.

The three most *fundamental* methods of distance measurements which do not need to be calibrated by other methods and which are not dependent on any a priori assumptions are: trigonometric parallaxes, stellar stream parallaxes, and Baade-Wesselink parallaxes of pulsating stars, preferably Cepheids. Unfortunately, nature did not provide us with classical Cepheids in globular clusters. Regarding trigonometric parallaxes, the satellite HIPPARCOS was designed to solve all problems. However, things turned out to be more complicated, mainly due to the fact that most interesting targets, for instance Cepheids, have large parallax errors even in the HIPPARCOS catalogue. There is already some controversy on that subject [53] and we shall not pursue it here. See Robichon et al. [40] for the most recent results on open cluster distances from HIPPARCOS measurements. The second method, using stellar stream parallaxes, is anyway reasonably applicable only to the Hyades cluster. To our knowledge, HIPPARCOS proper motions has yet to be used to derive a stream parallax to another cluster.

So we are left with Baade-Wesselink parallaxes. The principle of this method is to compare the pulsational radial velocity curve of a pulsating star with its light curve. In the black-body approximation,  $L \sim R^2 \cdot T_{\text{eff}}^4$  where  $L$ ,  $R$ ,  $T_{\text{eff}}$  are the absolute bolometric luminosity, the radius, and the effective temperature of the star, respectively. If  $r$  and  $L_{\text{app}}$  are the distance and apparent luminosity, respectively, we have  $L_{\text{app}} \cdot r^2 \sim L$ , and thus  $L_{\text{app}} \sim T_{\text{eff}}^4 \cdot (R/r)^2$ . But  $R/r$  is the angular diameter of the star and therefore the integration over the radial velocity curve gives the linear diameter and thus the distance, once  $T_{\text{eff}}^4$  can be determined. However, the practical application bears complications. Stars are not black-bodies, and the ability to measure  $T_{\text{eff}}$  by any observable parameter, for instance a colour index, was in former times often a question for the theory of stellar atmospheres. Meanwhile there is a sufficient number of interferometrically measured angular diameters of stars that there is no need to borrow any assumption from theory. According to our assessment, a variation of this method, known as the ‘‘Barnes-Evans method’’, which is essentially the adaptation for observational terminology, is the most promising approach today. Gieren et al. [14] applied this method in the infrared to 16 Galactic Cepheids to calibrate the period-luminosity relationship (PLR). With this PLR, they derive a distance modulus of  $18.46 \pm 0.05$  mag for the LMC. Infrared data already exist for LMC Cepheids in order to apply the Barnes-Evans method to these stars directly, but at the time of writing (February ’99) the results are not yet published. Work in the optical has been done by Gieren et al. [13], who applied the Barnes-Evans method to Cepheids in NGC 1866, a young globular cluster in the LMC. The result is in very good agreement with the result

from the PLR analysis. Admittedly, one still finds values between 18.2 and 18.7 mag for the LMC distance modulus in the literature, but the evaluation of these extreme values is beyond our scope. However, it is important to keep in mind that the LMC is the standard for extragalactic distances. With  $\mu_{\text{LMC}} = 18.46 \pm 0.06$  mag, we derive a zero-point for (4) of  $\beta = 0.53 \pm 0.12$ , based on the RR Lyrae brightnesses by Walker [60] and the globular cluster horizontal branches by Suntzeff et al. [54].

With this zero-point, we can now determine the absolute brightness of the TOM of the Galactic system, for which we use the ‘‘McMaster Catalogue’’ of Galactic GCs [19]. For the analytical representation, a Gaussian has often been used. But a close inspection of the LFs of the Galaxy, M31 and several GCLFs of Virgo ellipticals [51,52] even reveals that the GCLF is better described by a  $t_5$  function, which is analytically written as

$$t_5(m; m^0, \sigma_t) = \frac{8}{3\sqrt{5}\pi\sigma_t} \left( 1 + \frac{(m - m^0)^2}{5\sigma_t^2} \right)^{-3} \quad (5)$$

parameterised by the TOM  $m^0$  and the width  $\sigma_t$ . These parameters can be fitted to a given sample most precisely by the maximum-likelihood method [6].

**Table 3.** The TOMs of the Galactic globular cluster system in  $B$ ,  $V$  and  $I$ . The GC sample suffers in  $B$  and  $I$  from selection effects in the photometry data. Therefore the  $B$  and  $I$  TOMs are derived from the  $V$  TOM and the mean Galactic GCS colours  $\langle B - V \rangle$  and  $\langle V - I \rangle$ .

	$B$	$V$	$I$
$M^0$	$-6.85 \pm 0.10$	$-7.61 \pm 0.08$	$-8.48 \pm 0.10$
$\sigma_t$	$1.06 \pm 0.07$	$0.92 \pm 0.07$	$0.85 \pm 0.06$

## 4 The absolute brightness of type Ia supernovae

Concentrating our view on Ia SNe in early-type galaxies instead of spirals entails not only advantages. A disadvantage is that we have as targets only early-type galaxies, and since Ia events apparently avoid elliptical and S0 galaxies, the number of targets is relatively small. On the other hand, the advantage of early-type galaxies is their low dust content, whereas in spiral galaxies, the dust extinction is a notorious nuisance for both Cepheids and SNe. A further advantage is that globular clusters are brighter than Cepheids, making the method reach further in distance. Moreover, suitable SNe must be *well observed*. This means that the maximum should be covered and that the SN preferentially should be observed with a CCD to take account of

the galaxy background. However, many SNe in the HST Cepheid programme (see the Appendix) are *not* well observed and if one includes an object like SN 1937C in IC 4182 (which was the first SN with good spectra), one has to face controversial historical reconstruction of the light curve.

In what follows, we distinguish between SNe in the Fornax cluster and SNe in other elliptical galaxies.

#### 4.1 Type Ia supernovae in the Fornax cluster

During the last decades, the literature on the Virgo cluster as an extragalactic distance standard has grown to an uncomfortably complicated level. We now know that much of the controversy between the “long” and the “short” distance scale has to do with the fact that the Virgo cluster possesses a complicated substructure and an appreciable depth of  $\approx 15\%$  of its distance.

The Fornax cluster in the southern hemisphere is situated at a similar distance as the Virgo cluster, but its properties are quite different, making it much more appropriate as a distance standard. First, it is a compact, evolved galaxy cluster with only a small depth structure. Secondly, it is dominated by elliptical rather than spiral galaxies, alleviating problems with extinction. Thirdly, 3 Ia SNe have been observed since 1980. See Table 4 for details. In particular, SN 1992A in NGC 1380 is one of the best ever observed Ia events. The two other Fornax SNe both appeared in NGC 1316, a peculiar S0 galaxy, perhaps a merger, with a lot of small-scale dust structure. But only SN 1980N is well observed. We caution that the maximum phase of SN 1981D in  $V$  is documented by a single measurement only, which makes the colour quite uncertain.

**Table 4.** Type Ia SNe in the Fornax galaxy cluster. The photometry is taken from Hamuy et al. [17,18]. The data from SN 1981D result from our own light-curve fitting (small differences to the values reported in [38] result from slight differences in the fit procedure and demonstrate the lower quality of 81D).

SN	host galaxy	$B_{\max}$	$V_{\max}$	$I_{\max}$	$\Delta m_{15}$	$B - V$
1992A	NGC 1380	12.57	12.55	12.80	1.47	0.02
1980N	NGC 1316	12.49	12.44	12.70	1.28	0.05
1981D	NGC 1316	12.66	12.36	—	1.18	0.30

We now need the distance to the Fornax cluster in order to convert the apparent magnitudes in Table 4 into absolute magnitudes. In the next paragraphs, we discuss the Fornax cluster distance derived by GCLFs and other methods.

**Elliptical galaxies in the Fornax cluster** The first distance of the Fornax cluster based on GCLFs with CCD data was determined by Kohle et al. [26].

They analysed the globular cluster systems of 4 ellipticals in Fornax, not including the S0 host galaxies. Table 5 lists the apparent magnitudes of the TOMs together with the values  $\Delta V$ ,  $\Delta I$ , then corrections due to metallicity differences.

**Table 5.** Turn-over magnitudes of galaxies in the Fornax cluster.

galaxy	TOM( $V$ )	$\Delta V$	TOM( $I$ )	$\Delta I$
NGC 1374	$23.52 \pm 0.14$	0.22	$22.60 \pm 0.13$	0.09
NGC 1379	$23.68 \pm 0.28$	0.40	$22.54 \pm 0.34$	0.15
NGC 1427	$23.78 \pm 0.21$	0.12	$22.31 \pm 0.14$	0.06
NGC 1399	$23.90 \pm 0.08$	0.12	$22.36 \pm 0.06$	0.06

The metallicity correction is quite important because it accounts for the systematic metallicity difference between early-type galaxies and our reference, the Galaxy. This has the following background: as we have argued, the universal feature behind the luminosity function is the mass function. But at a given mass, globular clusters of different metallicities also have different luminosities, the metal-poorer ones being brighter. This is a well known and well understood property of stellar models and consequently also of stellar systems. The Galactic GCS comprises clusters with a wide variety of metallicities. Being a spiral galaxy, only a few of its clusters belong to the metal-rich bulge, the vast majority belong to the metal-poor halo. This is different for elliptical galaxies, where the bulges are the dominating structure components and, consequently, most GCs of elliptical galaxies are metal-rich. One should remark that it is not clear whether “halos” of early-type galaxies exist. Only in the case of the S0 galaxy NGC 1380, one of our host galaxies, has it been possible to distinguish between a “bulge” and a “halo” population [25]. However, it is plausible that the proportion of metal-rich to metal-poor GCs is in the case of elliptical galaxies much more in favour of metal-rich objects. Since it is not feasible to measure metallicities for individual GCs in ellipticals, one uses the *mean* colour of a GCS as a measure of the mean metallicity and calculates a corresponding correction, if the GCS under investigation has a different metallicity distribution. This can easily be done by using stellar models. Ashman & Zepf [3] provide tables where the relevant correction can be read off.

The application of that correction is however only reasonable if the TOM can be derived with an adequate accuracy. For that reason, we skip the quite uncertain case of NGC 1379 when calculating the error-weighted mean distance modulus from Table 5. Including the metallicity corrections, we derive a mean distance modulus of  $31.30 \pm 0.13$  mag in  $V$  and  $30.89 \pm 0.08$  mag in  $I$  for the elliptical galaxies of Kohle et al. [26]. The value derived from the  $I$  data is too small compared to the  $V$ -data value and the distance moduli from other methods presented later on. It is likely that the  $I$  images were not

deep enough and gave a wrong TOM. We therefore do not take this value into account.

Recently, Grillmair and co-authors [16] used the Hubble Space Telescope to obtain luminosity functions in  $B$  for NGC 1399, NGC 1404 and NGC 1316 (which is a special case and will be discussed shortly). The resulting distance modulus values (using our Milky Way TOMs) are  $31.41 \pm 0.11$  mag ( $B$ ) and  $31.34 \pm 0.11$  mag ( $V$ ) for NGC 1399, and  $31.69 \pm 0.23$  mag ( $B$ ) for NGC 1404. While the values for NGC 1399 confirm the TOMs from Table 5, the value for NGC 1404 is also in agreement with earlier work by Richtler et al. [37]. Although not entirely conclusive, this would set NGC 1404 out of the core of the Fornax cluster, which is suggested also by its strongly deviating radial velocity and its low specific frequency of globular clusters. Note, however, that surface-brightness fluctuations do not confirm the larger distance for NGC 1404 [24]. This issue remains open.

**NGC 1380, host galaxy for SN 1992A** As already mentioned, SN 1992A is one of the best ever observed Ia SNe and therefore enters the zero point determination of the Ia Hubble diagram with a high weight. The GCS of NGC 1380 has been analysed by Kissler-Patig et al. [25] and Della Valle et al. [10]. Interestingly, it turned out that the GCS could be separated into an elongated metal-rich bulge and a spherical, metal-poor halo population.

Due to the excellent data quality (very long exposed NTT data in very good seeing conditions) it was possible to trace the luminosity function 1 mag below the TOM, and thus the GCS of NGC 1380 is the deepest observed GCS from ground-based data. Table 6 lists the apparent brightnesses and the widths of the  $t_5$ -functions for  $B$ ,  $V$ , and  $I$ . The metallicity corrections are negligible in this case.

**Table 6.** Listed are the apparent TOMs and  $\sigma_t$ -values of the  $t_5$ -functions representing the GCS of NGC 1380 in the bands  $V$ ,  $B$ , and  $R$  according to Della Valle et al. [10]

Filter	TOM	$\sigma_t$
$B$	$24.38 \pm 0.09$	$0.89 \pm 0.10$
$V$	$23.69 \pm 0.11$	$0.95 \pm 0.10$
$R$	$23.17 \pm 0.10$	$0.98 \pm 0.10$

**NGC 1316, host galaxy to SN 1980N and SN 1981D** The fact that NGC 1316 hosted two Ia's (photometry can be found in Hamuy et al. [17]), gives it a particular character. However, it is not the perfect standard it could be. First, SN 1981D is not very well observed, in particular the  $V$ -peak maximum has a large error, making the colour and the corresponding



corrections uncertain. Secondly, NGC 1316 is not a well behaved elliptical galaxy, but is classified as a peculiar S0 galaxy, suspected to have been formed in its present shape in a merger. It is known that globular clusters can form in large numbers in galaxy mergers. If this event had happened, say,  $10^9$  years ago [50], and a lot of globular clusters had been formed, we would expect a TOM (if any) at distinctly fainter magnitudes than in the case of the other Fornax ellipticals, because of the many intermediate-age globular clusters.

In fact, Grillmair et al. [16] in their HST study see no TOM at all, but an exponential increase of sources beyond the magnitude where the TOM could be expected. They suggest these sources could be many younger open clusters formed in the merger, but then apparently not many bright globular clusters could have been formed.

At the time of writing we [15] are undertaking a study of this GCS. Preliminary results are compatible with the results found by Grillmair et al. [16] (at least down to  $V \sim 24$  mag) in the central region, which we cannot access with ground-based data. We found a  $V$ -TOM of 23.7 mag for the entire LF, which fits well to the other Fornax ellipticals. But we found different  $V$ -TOM's for our inner (23.7 mag) and outer (24.3 mag) regions. If the TOM's were modified by additional young clusters formed in the merger, one would have expected the reverse.

It is also curious that the number of clusters is extremely low for such a bright galaxy. Regarding the nature of the cluster system, this galaxy is very interesting, but it is not clear how reliable the GCLF is as a distance indicator. Planetary nebulae remain another possibility to derive a distance (see below).

**Fornax cluster distances from other methods** The method of GCLFs which we pursue here is of course not the only way to determine the Fornax cluster distance. Even if we have no space to go into details, it is very interesting to have a quick look at other means and see what they arrive at.

*Cepheids* The core of the Fornax cluster does not contain spiral galaxies, in which Cepheids can be found. NGC 1365, a large barred spiral galaxy, is situated well outside the core. The HST has been used to find Cepheids and to derive a distance based on the period-luminosity relation. Madore et al. [30] quote a distance modulus of  $31.35 \pm 0.07$  mag.

*Surface brightness fluctuations* The method of “surface brightness fluctuations” is applicable to early-type galaxies and bulges of spiral galaxies. It uses the fact that the pixel-to-pixel variation in a CCD image of an elliptical galaxy is not simply the photon noise but depends in a characteristic manner on the surface density of (unresolved) red giants. With increasing galaxy distance, an increasing number of individual red giants are covered by one pixel and the “surface brightness fluctuations” from pixel to pixel become smaller,

approaching pure photon noise. This effect is particularly pronounced in the infrared region.

Jensen et al. [24] give distances for 6 elliptical galaxies in the Fornax cluster. Their average distance modulus is 31.36 mag. It is interesting that NGC 1404 fits well with the other ellipticals, in mild contrast to its GCLF.

*Planetary Luminosity Functions* Planetary nebulae can easily be identified in early-type galaxies through narrow-band photometry with filters centred on emission lines. The assumption that the luminosity function of planetary nebulae (PNLF) is universal qualifies PNLFs as distance indicators in a similar manner as GCLFs.

McMillan et al. [33] quote  $31.14 \pm 0.14$  mag as the mean distance modulus for NGC 1316, NGC 1399, and NGC 1404. However, this is based on an Andromeda distance modulus value about 0.2 mag smaller than the modern Cepheid value of M31. It also supports the assumption that NGC 1316 (as a Ia host galaxy) is at the same distance as the Fornax core. The excellent agreement of the PNLF distance with the GCLF distance (although numerically a bit coincidental) is very satisfactory and moreover is a strong point for the universality of the GCLF.

**Absolute brightness of Fornax SNe** We now can calculate the absolute brightness of the Fornax supernovae by applying decline-rate and colour corrections according to (3) and the values of Table 4. Using the distance modulus of  $\mu_{\text{Fornax}} = 31.35$  mag for all SNe in the Fornax Cluster, we obtain the values listed in Table 7.

**Table 7.** The corrected absolute brightnesses of SNe in the Fornax galaxy cluster.

SN	Host Galaxy	$M_{B,\text{cor}}$	$M_{V,\text{cor}}$	$M_{I,\text{cor}}$
1992A	NGC 1380	$-18.99 \pm 0.16$	$-19.01 \pm 0.16$	$-18.69 \pm 0.16$
1980N	NGC 1316	$-19.02 \pm 0.16$	$-19.04 \pm 0.16$	$-18.74 \pm 0.16$
1981D	NGC 1316	$-19.20 \pm 0.23$	$-19.28 \pm 0.24$	—

## 4.2 Ia events in early-type galaxies outside the Fornax cluster

Not many Ia SNe outside the Fornax cluster are currently known for which we could measure reliable distances via GCLFs. Either the SN is badly observed or the host galaxy has not yet been a target regarding its GCLF, or planetary nebulae, or surface brightness fluctuations (see the compilation of Della Valle et al. [10]). Primarily, this is SN 1994D in the S0 galaxy NGC 4526 [36], located in the southern extension of the Virgo cluster. This supernova is an interesting case because it has been suspected to violate the decline-rate–luminosity relation by being too bright in spite of an overall completely

normal photometric and spectroscopic behaviour [36,45]. However, our GCLF distance to NGC 4526 [11] was the first published individual distance determination for this galaxy, which shows that NGC 4526 lies in the foreground of the Virgo cluster. We derived a distance modulus of  $30.4 \pm 0.3$  mag.

Another interesting galaxy is NGC 4374 which hosted 3 Ia’s! Unfortunately, this is not of great value for us. SN 1957B is too badly observed, as is SN 1980I (this latter SN is sometimes labelled “extragalactic”, located almost in the middle between NGC 4374 and NGC 4406. The third one, SN 1991bg, is very well observed but is quite peculiar [18]. It is one of the faintest and reddest Ia events ever observed and probably cannot enter the Hubble constant determination currently with any weight. Moreover, the distance for NGC 4374 is not yet conclusive. A GCLF for NGC 4374 has been determined by Ajhar et al. [1]. They give a TOM in the  $R$ -band of 23.58 mag. Using  $-8.14$  mag as the Galactic TOM in  $R$ , one obtains 31.72 mag as the distance modulus. With this distance for NGC 4374, it is interesting that the corrections for decline rate and colour shift even this weird SN into a domain where its corrected brightness is comparable to that of the Fornax SNe. The error is huge, admittedly, but this is a consequence of the large and uncertain colour correction, because the respective fit has been done over a small colour interval only. However, it must be cautioned that the distance value based on planetary nebulae is smaller [23], leading to a brightness which is definitely too small to be compatible with other Ia SNe.

Table 8 lists the resulting absolute magnitudes for SN 1994D and SN 1991bg. The fact that for SN 1991bg the absolute magnitudes differ strongly from colour to colour is evidence that the colour correction must be improved before such a strong extrapolation can be reasonably done.

**Table 8.** Listed are the relevant parameters and absolute corrected brightnesses for SN 1994D and SN 1991bg based on the distance determinations quoted in the text.

SN	$\Delta m_{15}$	$B_{\max} - V_{\max}$	$M_{B,\text{cor}}$	$M_{V,\text{cor}}$	$M_{I,\text{cor}}$
1994D	$1.31 \pm 0.08$	$-0.05 \pm 0.04$	$-18.69 \pm 0.31$	$-18.69 \pm 0.31$	$-18.44 \pm 0.31$
1991bg	$1.93 \pm 0.10$	$0.79 \pm 0.11$	$-18.55 \pm 0.56$	$-18.83 \pm 0.49$	$-19.18 \pm 0.50$

Another “peculiar” Ia SN, which, according to its probable distance of the host galaxy, turns out to be too bright, is SN 1991T in NGC 4527 (e.g. [18]). Although its photometric behaviour is normal, NGC 4527 should have a distance modulus of about 29.90 mag to bring SN 1991T in agreement with other SNe. A Cepheid distance to this galaxy would be very desirable.

## 5 The Hubble constant and conclusions

Since there is no standardisation yet either in Cepheid distances, globular cluster distances, fit procedures etc., one must be aware that the actually derived Hubble constant is sensitive to all these individual assumptions and uncertainties. When calculating a Hubble constant value from SN data it is necessary to assign weights according to the observational quality of individual SNe. To keep things as easy as possible, we calculated the Hubble constant values for all SNe (except SN 1991bg) in each filter and then adopt one value for each SN as listed in Table 9. The individual values cannot be simply averaged because they are not independent. After properly averaging the adopted values we get a resulting Hubble constant of  $72 \pm 4 \text{ km s}^{-1} \text{ Mpc}^{-1}$ .

**Table 9.** The Hubble constant values are calculated for 4 SNe in each filter according to (2) with the data from Tables 2, 7, and 8.

SN	$H_{0,B}$	$H_{0,V}$	$H_{0,I}$	$H_0$ (adopted)
1992A	$73.0 \pm 5.4$	$72.8 \pm 5.4$	$74.2 \pm 5.5$	$73 \pm 6$
1980N	$72.0 \pm 5.3$	$71.8 \pm 5.3$	$72.5 \pm 5.3$	$72 \pm 6$
1981D	$66.3 \pm 7.0$	$64.3 \pm 7.1$	—	$65 \pm 7$
1994D	$83.8 \pm 11.6$	$84.3 \pm 12.0$	$83.2 \pm 11.9$	$84 \pm 12$

## 6 Appendix: Type Ia SNe in spiral galaxies

Though this article deals primarily with SNe in early-type galaxies, the major part of the literature on Ia SNe as distance indicators is related to spiral galaxies. First, this is simply due to the fact that the Ia rate in spirals is larger, but secondly also because of the attractive possibility of identifying Cepheids with the Hubble Space Telescope and deriving accurate distances by means of the period-luminosity relation. Our approach to the Hubble constant would thus be incomplete to an intolerable level if we would not briefly consider Ia's in late-type galaxies and compare them with those in early-type galaxies. Rather than discussing the literature, we shall re-derive distances and absolute supernova magnitudes in the same way as we have done for SNe in early-type galaxies. For that we set readability and didactic argumentation at low priority. The results will be squeezed into a few tables, which then have the character of an appendix.

### 6.1 The method of deriving distances

Some Ia events occurred in nearby spiral galaxies, where the Hubble Space Telescope could detect and measure Cepheids.

We mainly encounter two difficulties. For the older SNe, the problem lies with the photometry of the given SN rather than with the distance of the host galaxy. For example, a SN like SN 1895B in NGC 5253 is not suitable because of its uncertain photometry. Sometimes, the light curve is more a matter of historical reconstruction than of exact measurements, for instance in the case of SN 1937C [35]. We are left with only a handful of promising targets, see Table 10. But even among those, not all light curves are convincingly reliable, especially those observed in the pre-CCD era, because diaphragm photometry does not allow the subtraction of the local background, which in the case of spiral galaxies with their small-scale variations is more important than for early-type galaxies. The second difficulty is the uncertain extinction towards the SNe and the Cepheids. All Cepheid observations with HST have employed the  $V$  and  $I$  filters, but only two of all SN light curves which come here into question are given in  $I$ , where the extinction is smallest.

To be consistent in the distance scale, we re-derived all distance moduli on the basis of published Cepheid photometry. We cannot discuss all SNe in detail and refer the reader to the cited literature. For each Cepheid in a given galaxy, we compute its  $m - M$ -value by applying the P-L-relations [14]

$$\begin{aligned} M_V &= -2.769 \cdot \log P/d - 1.294 \\ M_I &= -3.041 \cdot \log P/d - 1.726 \end{aligned} \quad (6)$$

and take the mean for all Cepheids. Sometimes, it seems reasonable to skip individual Cepheids, because of a too striking deviation. A respective remark is given in these cases. We obtain a larger magnitude difference  $m - M$  in  $V$  than in  $I$  except for IC 4182. In principle, this difference for  $V$  and  $I$  is interpreted as a difference in the mean extinction. We now have to assume a universal reddening law (which can be erroneous), and calculate the extinction according to  $A_{B,V,I} = R_{B,V,I} \cdot E(V - I)$ , where  $R_{B,V,I}$  takes the values, 2.56, 1.93, 0.93, respectively [39]. The errors  $\Delta(m - M)_V$  and  $\Delta(m - M)_I$  are the dispersions of the individual Cepheid values divided by the square root of the number of Cepheids. From  $(m - M)_V - A_V = (m - M)_I - A_I$  and the mean reddening  $E(V - I) = (m - M)_V - (m - M)_I$  we obtain the distance modulus  $\mu = R_V \cdot (m - M)_I - R_I \cdot (m - M)_V$ . Note that  $R_V - R_I = 1$  by definition.

Table 10 lists those SNe which come into question. Van den Bergh [59] is a useful reference for a compilation of most of the data. We did not include SN 1998bu in NGC 3368 (M96) [55] because of its red colour at maximum light. This supernova is clearly reddened but the relative contributions of reddening and intrinsic colour remain uncertain.

The distance moduli quoted in Table 11 normally do not differ much from the values given in the literature. In a few cases, differences may amount to about 0.2 mag, depending on the details of the Cepheid selection which can influence the adopted extinction.

The data in Table 12 are the necessary input for computing the *corrected* absolute magnitudes of the SNe as we have done for the SNe in early-type

**Table 10.** This table lists the suitable Ia events in late-type galaxies where the distance can be derived from Cepheids.

SN	Host galaxy	Ref. for SN	Ref. for Cepheids
1937C	IC 4182	[35]	[41]
1960F	NGC 4496	[48]	[43]
1972E	NGC 5253	[18]	[42]
1974G	NGC 4414	[49]	[57]
1981B	NGC 4536	[47]	[44]
1990N	NGC 4639	[17]	[46]

**Table 11.** Listed are the number of Cepheids used for the distance determination, the magnitude difference  $m - M$  for  $V$  and  $I$ , the resulting reddening (the difference of the distance moduli for IC 4182 is negative!), the extinction-corrected distance moduli, and remarks regarding details of the Cepheid selection.

Host gal.	#	$(m - M)_V$	$(m - M)_I$	$E(V - I)$	$\mu$	Remarks
IC 4182	27	$28.21 \pm 0.05$	$28.31 \pm 0.05$	0 (def.!)	$28.26 \pm 0.07$	
NGC 4496	31	$31.06 \pm 0.05$	$30.97 \pm 0.05$	$0.09 \pm 0.07$	$30.89 \pm 0.11$	
NGC 5253	8	$27.99 \pm 0.07$	$27.77 \pm 0.12$	$0.20 \pm 0.14$	$27.57 \pm 0.24$	1
NGC 4414	8	$31.43 \pm 0.09$	$31.36 \pm 0.08$	$0.07 \pm 0.12$	$31.30 \pm 0.17$	2
NGC 4536	31	$31.07 \pm 0.05$	$30.97 \pm 0.05$	$0.10 \pm 0.07$	$30.89 \pm 0.11$	
NGC 4639	8	$31.71 \pm 0.08$	$31.68 \pm 0.05$	$0.03 \pm 0.09$	$31.65 \pm 0.12$	3

1: largest period skipped. 2: smallest modulus skipped. 3: largest modulus skipped, perhaps differential reddening, best Cepheids selected

galaxies. Then we calculate the corresponding values of the Hubble constant according to (2). The results are given in Table 13.

We expect from the Hubble diagram of the Calán/Tololo sample that the scatter among the corrected magnitudes is of the order 0.1 mag. We therefore do not interpret the large scatter of, for example in  $M_B$ , 0.9 mag as being real, but being due to errors. The distances are in most cases well determined, one may rather suspect the photometry of the SNe to be unreliable. Because we know from the Calán/Tololo and CfA-sample that SNe in early-type galaxies and late-type galaxies are indistinguishable after the appropriate corrections, we presume that SN 1974G and SN 1960F are the problematic cases. In fact, both are SNe with considerable photometric uncertainties. In the case of SN 1960F, the  $V$  magnitude at maximum is not well constrained, which gives much freedom with respect to the colour correction.

When we skip these two SNe, the Hubble constant (in  $\text{km s}^{-1} \text{Mpc}^{-1}$ ) for  $B$ ,  $V$  and  $I$  results to be  $72.0 \pm 2.3$ ,  $72.9 \pm 2.5$ , and  $73.4 \pm 6.7$ . We emphasise that these errors are of “internal” nature, i.e. they measure the uncertainty of the applied method. The uncertainty resulting from a possible error in the distance scale is not included. However, one can regard all Cepheid distances as being based on a distance modulus of the Large Magellanic Cloud of 18.50 mag. An increase of 0.1 mag approximately results in a decrease of

3 km s<sup>-1</sup> Mpc<sup>-1</sup> of the Hubble constant value. Infrared Barnes-Evans distances to LMC Cepheids will probably give the most accurate values in the near future.

**Table 12.** This table lists the apparent brightnesses (not extinction corrected) of our SNe together with the adopted reddening and the decline rate. See Van den Bergh [59] for a discussion of the relevant literature.

SN	$B_{\max}$	$V_{\max}$	$I_{\max}$	$E(B - V)$	$\Delta m_{15}$
1937C	$8.94 \pm 0.03$	$9.00 \pm 0.03$	–	0.0	$0.85 \pm 0.10$
1960F	$11.77 \pm 0.07$	$11.51 \pm 0.18$	–	$0.06 \pm 0.04$	$1.06 \pm 0.08$
1972E	$8.49 \pm 0.14$	$8.49 \pm 0.15$	$8.80 \pm 0.19$	$0.05 \pm 0.02$	$0.87 \pm 0.10$
1974G	$12.48 \pm 0.05$	$12.30 \pm 0.05$	–	$0.16 \pm 0.07$	$1.11 \pm 0.06$
1981B	$12.04 \pm 0.04$	$12.00 \pm 0.07$	–	0.0	$1.10 \pm 0.05$
1990N	$12.74 \pm 0.03$	$12.72 \pm 0.03$	$12.95 \pm 0.05$	0.0	$1.07 \pm 0.05$

**Table 13.** Given are the absolute *corrected* magnitudes, and the corresponding Hubble constant values as derived with (2) and the coefficients from Table 2.

SN	$M_{B,\text{cor}}$	$M_{V,\text{cor}}$	$M_{I,\text{cor}}$
1937C	$-19.11 \pm 0.10$	$-19.08 \pm 0.11$	–
1960F	$-19.61 \pm 0.31$	$-19.68 \pm 0.36$	–
1972E	$-19.07 \pm 0.35$	$-19.05 \pm 0.38$	$-18.72 \pm 0.30$
1974G	$-19.41 \pm 0.23$	$-19.43 \pm 0.23$	–
1981B	$-18.91 \pm 0.16$	$-18.92 \pm 0.17$	–
1990N	$-18.93 \pm 0.12$	$-18.93 \pm 0.14$	$-18.70 \pm 0.25$
SN	$H_{0,B}$	$H_{0,V}$	$H_{0,I}$
1937C	$69.1 \pm 3.2$	$70.5 \pm 3.6$	–
1960F	$54.9 \pm 7.8$	$53.5 \pm 8.9$	–
1972E	$70.3 \pm 11.3$	$71.4 \pm 12.5$	$73.0 \pm 10.5$
1974G	$60.1 \pm 6.4$	$60.0 \pm 6.3$	–
1981B	$75.7 \pm 5.6$	$75.9 \pm 5.9$	–
1990N	$75.0 \pm 4.1$	$75.5 \pm 4.9$	$73.7 \pm 8.6$

## References

1. Ajhar E.A., Blakeslee J.P., Tonry J.L. (1994) *VRI* photometry of globular clusters in Virgo and Leo ellipticals. AJ 108,2087
2. Arnett W.D., Bahcall J.A., Kirshner R.P., Woosley S.E. (1989) Supernova 1987A. ARAA 29,629
3. Ashman K.M., Conti A., Zepf S.E. (1995) Globular Cluster Systems as Distance Indicators Metallicity Effects on the Luminosity Function. AJ 110,1164

4. Barbon R., Buondi V., Capellaro E., Turatto M. (1999) The Asiago Supernova Catalogue-10 years after. astro-ph/9908046, <http://athena.pd.astro.it/~supern/>
5. Bartunov O.S., Tsvetkov D.Y., Filimonova I.V. (1994) Distribution of supernovae relative to spiral arms and H II regions. *PASP* 106,1276
6. Bevington P.R., Robinson D.K. (1992) *Data Reduction and Error Analysis for the Physical Sciences*. McGraw-Hill, 2nd Edition
7. Branch D. (1998) Type Ia supernovae and the Hubble constant. *ARAA* 36,17
8. Cappellaro E., Turatto M., Benetti S., Tsvetkov D.Y., Bartunov O.S., Makarova I.N. (1993) The rate of supernovae II. The selection effect and the frequencies per unit blue luminosity. *A&A* 273,383
9. Colgate S.A., McKee C. (1969) Early Supernova Luminosity. *ApJ* 157, 623
10. Della Valle M., Kissler-Patig M., Danziger J., Storm J. (1998) Globular cluster calibration of the peak brightness of the type Ia supernova 1992A and the value of  $H_0$ . *MNRAS* 299,267
11. Drenkhahn G., Richtler T. (1999) SN1994D in NGC 4526: a normally bright type Ia supernova. *A&A*, in press
12. Filippenko A.V. (1997) Optical Spectra of Supernovae. *ARAA* 35,309
13. Gieren W.P., Richtler T., Hilker M. (1994) The distance to the Large Magellanic Cloud cluster NGC 1866 from its Cepheid members. *ApJ* 433,L73
14. Gieren W.P., Fouqué P., Gomez M. (1998) Cepheid Period-Radius and Period-Luminosity Relations and the Distance to the Large Magellanic Cloud. *ApJ* 496,17
15. Gómez M., Richtler T., Infante L., Drenkhahn G., (1999) The peculiar globular cluster system of NGC 1316 (Fornax A). *AGM* 15,P62
16. Grillmair C.J., Forbes D.A., Brodie J.P., Elson R.A.W. (1999) HST imaging of the globular clusters in the Fornax cluster: color and luminosity distribution. *AJ* 117,167
17. Hamuy M., Phillips M.M., Maza J., Wischnjewsky M., Uomoto A., Landolt A.U., Khatwani R. (1991) The optical light curves of SN 1980D and SN 1981N in NGC 1316 (Fornax A). *AJ* 102,208
18. Hamuy M., Phillips M.M., Suntzeff N.B., Schommer R.A., Maza J., Aviles R., (1996) The Hubble diagram of the Calán/Tololo type Ia supernovae and the value of  $H_0$ . *AJ* 112,2398
19. Harris W.E. (1996) A Catalog of Parameters for Globular Clusters in the Milky Way. *AJ* 112,1487, <http://physun.physics.mcmaster.ca/Globular.html>
20. Heithausen A., Bensch F., Stutzki J., Falgarone E., Panis J.F. (1998). The IRAM key project: small-scale structure of star forming regions. Combined mass spectra and scaling laws. *A&A* 331,L65.
21. Heithausen A., Stutzki J., Bensch F., Falgarone E., Panis J.F. (1998). Results from the IRAM key project: "The small-scale Structure of Pre-star-forming Regions" laws. *Rev. of Mod. Astron.* 12,101
22. Höflich P., Khokhlov A., Wheeler J.C., Phillips M.M., Suntzeff N.B., Hamuy M. (1996) Maximum Brightness and Postmaximum Decline of Light Curves of Type Ia Supernovae: A Comparison of Theory and Observations. *ApJ* 472,L81
23. Jacoby G.H., Ciardullo R., Ford, H.C. (1990) Planetary nebulae as standard candles. V - The distance to the Virgo Cluster. *ApJ* 356,332
24. Jensen J.B., Tonry J.L., Luppino G.A. (1988) Measuring Distances Using Infrared Surface Brightness Fluctuations. *ApJ* 505,111
25. Kissler-Patig M., Richtler T., Storm J., Della Valle M. (1997) Halo and bulge/disk globular clusters in the S0 galaxy NGC 1380. *A&A* 327,503



26. Kohle S., Kissler-Patig M., Hilker M., Richtler T., Infante L., Quintana H. (1996) The distance of the Fornax cluster based on globular cluster luminosity functions. *A&A* 309,L39
27. Kuchner M.J., Kirshner R.P., Pinto P.A., Leibundgut B. (1993) Evidence for Ni-56 yields Co-56 yields Fe-56 decay in type Ia supernovae. *ApJ* 426, L89
28. Kundt W. (1990) Supernova explosions and their ejected shells. In: Kundt W. (Ed.) *Neutron Stars and their Birth Events*. NATO ASI C300, Kluwer, p. 40
29. Kundt W. (1998) Astrophysics of neutron stars - facts and fiction about their formation and functioning. *Fund. of Cosm. Phys.* 20,1
30. Madore B.F., Freedman W.L., Silbermann N. et al. (1998) A Cepheid distance to the Fornax cluster and the local expansion rate of the Universe. *Nature* 395,47
31. McCray R. (1993) SN 1987A Revisited. *ARAA* 31,175
32. McLaughlin D.E. (1994) An analytical study of the globular cluster luminosity function. *PASP* 106,47
33. McMillan R., Ciardullo R., Jacoby G.H. (1993) Planetary nebulae as standard candles. IX. The distance to the Fornax cluster. *ApJ* 416,62
34. Phillips M.M. (1993) The absolute magnitudes of Type Ia supernovae. *ApJ* 413,L105
35. Pierce M.H., Jacoby G.H. (1995) "New" *B* and *V* photometry of the "old" type Ia supernova 1937C. *AJ* 110,2885
36. Richmond M.W., Treffers R.R., Filippenko A.V., Van Dyk S.D., Paik Y., Peng C., Marschall L.A., Laaksonen B.D., Macintosh B., McLean I.S. (1995) *UBVRI* Photometry of the Type Ia SN 1994D in NGC 4526. *AJ* 109,2121
37. Richtler T., Grebel E.K., Domgoergen H., Hilker M., Kissler M. (1992) The globular cluster system of NGC 1404. *A&A* 264,25
38. Richtler T., Drenkhahn G., Gómez M., Seggewiss W. (1999) The Hubble Constant from the Fornax Cluster Distance. In: *Science in the VLT era and beyond*. ESO VLT Opening Symposium. Springer-Verlag, Berlin, in press
39. Rieke G.H., Lebofsky M.J. (1985) The interstellar extinction law from 1 to 13 microns. *ApJ* 288,618
40. Robichon N., Arenou F., Mermilliod J.C., Turon C. (1999) Open clusters with Hipparcos. I. Mean astrometric parameters. *A&A* 345,471
41. Saha A., Labhardt L., Schwengeler H., Macchetto F.D., Panagia N., Sandage A., Tammann G.A. (1994) Discovery of Cepheids in IC 4182: Absolute peak brightness of SN 1937C and the value of  $H_0$ . *ApJ* 425,14
42. Saha A., Sandage A., Tammann G.A., Labhardt L., Schwengeler H., Panagia N., Macchetto F.D. (1995) Discovery of Cepheids in NGC 5253: Absolute peak brightness of SN 1895B and SN 1972E and the value of  $H_0$ . *ApJ* 438,8
43. Saha A., Sandage A., Labhardt L., Tammann G.A., Schwengeler H., Macchetto F.D., Panagia N. (1996) Cepheid calibration of the peak brightness of type Ia supernovae: SN 1960F in NGC 4496A. *ApJS* 107,693
44. Saha A., Sandage A., Labhardt L., Tammann G.A., Schwengeler H., Macchetto F.D., Panagia N. (1996) Cepheid calibration of the peak brightness of type Ia supernovae: SN 1981B in NGC 4536. *ApJ* 466,55
45. Sandage A., Tammann G.A. (1995) Steps toward the Hubble Constant. X. The Distance of the Virgo Cluster Core Using Globular Clusters. *ApJ* 446,1
46. Sandage A., Saha A., Tammann G.A., Labhardt L., Panagia N., Macchetto F.D. (1996) Cepheid Calibration of the Peak Brightness of Type Ia Supernovae: Calibration of SN 1990N in NGC 4639 Averaged with Six Earlier Type Ia Supernova Calibrations to Give  $H_0$  Directly. *ApJ* 460,15

47. Schaefer B.E. (1995) The peak brightness of SN 1981F in NGC 4536 and the Hubble constant. *ApJ* 449,L9
48. Schaefer B.E. (1996) The peak brightness of SN 1960F in NGC 4496 and the Hubble constant. *ApJ* 460,L19
49. Schaefer B.E. (1998) The peak brightness of SN 1974G in NGC 4414 and the Hubble constant. *ApJ* 509,80
50. Schweizer F. (1980) An optical study of the giant radio galaxy NGC 1316 (Fornax A). *ApJ* 237,303
51. Secker J. (1992) A statistical investigation into the shape of the globular cluster luminosity distribution. *AJ* 104,1472
52. Secker J., Harris W.E. (1993) A maximum likelihood analysis of globular cluster luminosity distributions in the Virgo ellipticals. *AJ* 105,1358
53. Seggewiss W. (1998) The distance scale of the Universe before and after Hipparcos. In: Brosche P., Dick W.R., Schwarz O., Wielen R. (Eds.) *The Message of the Angles - Astrometry from 1798 to 1998. Proc. of the International Spring Meeting of the Astronomische Gesellschaft Gotha 1998*, Verlag Harri Deutsch, Thun und Frankfurt am Main 1998, p. 150
54. Suntzeff N.B., Schommer R.A., Olszewski E.W., Walker A.R. (1992) Spectroscopy of giants in LMC clusters III. Velocities and abundances for NGC 1841 and reticulum and the properties of the metal-poor clusters. *AJ* 104,1743
55. Suntzeff N.B., Phillips M.M., Covarrubias R. et al. (1999) Optical lightcurve of the Ia supernova SN 1998bu in M96 and the supernova calibration of the Hubble constant. *AJ* 117,1175
56. Trimble V.L. (1982) *Supernovae: A Survey of Current Research, Part I: The Events. Reviews of Modern Physics. Vol. 54*
57. Turner A., Ferrarese L., Saha A. (1998) The Hubble Space Telescope project on the extragalactic distance scale: The Cepheids in NGC 4414. *ApJ* 505,207
58. VandenBerg D.A., Stetson P.B., Bolte M. (1996) The age of the Galactic globular cluster system. *ARAA* 34,461
59. Van den Bergh S. (1996) The luminosities of type Ia supernovae derived from Cepheid calibration. *ApJ* 472,431
60. Walker A.R. (1992) The absolute magnitudes of LMC RR Lyrae variables and the ages of Galactic globular clusters. *ApJ* 390,L81
61. Wang L., Höflich P., Wheeler J.C. (1997) *Supernovae and Their Host Galaxies. ApJ* 483,L29
62. Wheeler J.C., Harkness R.P. (1990) *Classification of Supernovae. In: Petschek A.G. (Ed.) "Supernovae". A&A Library, Springer 1990*
63. Whitmore B.C. (1996) *Globular Clusters as Distance Indicators. In: Livio M., Donahue M., Panagia N. (Eds.) The Extragalactic Distance Scale. STScI Symp. Ser. 10, Cambridge University Press*
64. Woosley S.E. (1990) *Type I Supernovae: Carbon Deflagration and Detonation. In: Petschek A.G. (Ed.) Supernovae. A&A Library, Springer, Ney York*

## 7 Acknowledgements

We thank Wilhelm Seggewiss for many useful discussions and the permission to use his literature compilation. We also thank Gordon Ogilvie for manuscript reading and Bruno Leibundgut for helpful and improving comments.